Impacts of the invasive hornet *Vespa velutina* on native wasp species: a first effort to understand population-level effects in an invaded area of Europe

L. Carisio[1], J. Cerri[2], S. Lioy[1], E. Bianchi[1], S. Bertolino[3], M. Porporato[1]

1 Department of Agriculture, Forest and Food Sciences, University of Turin, Largo Paolo Braccini 2, 10095 Grugliasco (Turin), Italy

2 Faculty of Mathematics, Natural Sciences and Information Technologies, University of Primorska, Glagoljaška 8, 6000 Koper, Slovenia

3 Department of Life Sciences and Systems Biology, University of Turin, Via Accademia Albertina 13, 10123 Turin, Italy

Supplementary material

Appendix S1

Introduction

In the following section, we will outline our approach to model selection, based on graphical causal models and the back-door criterion.

Model fitting for causal inference (Morgan & Winship, 2015) has the ultimate goal of quantifying the effect of a change in a treatment variable (X) over a response variable (Y). A causal effect of X over Y (X → Y) implies that a change in X determines a change in Y, while a change in Y does not produce any change in X. There are, of course, more refined definitions of causal effects, also involving counterfactuals, but we encourage you to read Morgan & Winship (2015) for a complete overview. The effect of X → Y can be estimated in three main ways:

- by carrying out a randomized experiment, where observations are randomly allocated to different treatments (different values of X);
- from field experiments, assuming that the allocation of observed units to treatment conditions is "as good as random" (e.g. instrumental variables, see Dunning, 2012);
- from observational data, when units are not allocated at random, but when confounding factors between X and Y are absent.

In these three situations, associations between variables are assumed to reflect the pure causal effect X → Y. There are two easy examples:

- in a treatment-control experiment, or in a field experiment (e.g. regression discontinuity design), the causal effect corresponds to the average treatment effect, the difference in the mean of the outcome variable (Y), between treated and non-treated units;
- in a study exploring the association between two continuous variables, where units are allocated at random between conditions with higher values of the X, the causal effect is reflected by a correlation coefficient (e.g. the Pearson's correlation coefficient) between the two variables.

When an association between variables is identified, this might be the result of the influence of a further variable (Z), which leads to an association by chance not reflecting a true causal effect between X and Y. The identification of a spurious association is called confounding.

An example of confounding is represented in Fig. S.1.

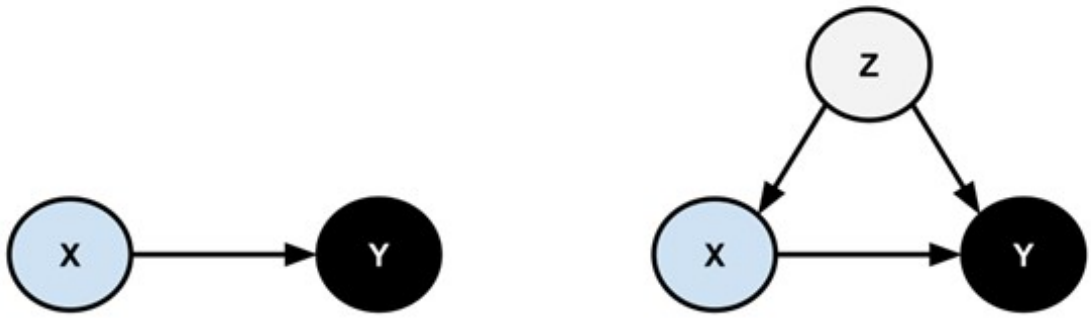

Fig. S.1 – On the left, the causal effect of X on Y can be identified (e.g. from an average treatment effect or a correlation coefficient), while on the right confounding from Z could make a covariation between X and Y arising by chance, and not reflecting X → Y.

While a proper randomized trial protects researcher against confounding, even from unobserved variables that they do not know, confounding can also be addressed when dealing with observational data. In observational studies, the levels of the X are not manipulated, but simply observed, like in our study. In that case, it is possible to make the partial correlation between X and Y representing X → Y, if all the relevant confounders (Z) are included as covariates in a multivariate model.

Our study aimed to estimate the causal effect of the abundance of the invasive hornet *Vespa velutina*, expressed as the number of individuals trapped per day per trap, over the abundance of the native hornet *Vespa crabro*. Ideally, a causal effect in which *V. crabro* abundances decline at higher densities of *V. velutina* would provide preliminary evidence for a competition between the two species. However, as our data are not manipulated, we need to:

1. include all the environmental covariates which could have influenced the number of catches at trapping sites, for the two species;
2. check for, and eventually account for, residual spatial correlation in our model;
3. evaluate model compatibility with the proposed causal structure.

In our case study, we implemented the first two steps without performing the last aspect for modelling reasons. There are some statistical methods that can tell whether the proposed causal structure is supported by the observed data (even though this does not reject alternative structures, see Bollen & Pearl, 2013) but they work only for some particular approaches, like

path analysis or Bayesian networks. These approaches were not suitable for our case study, characterized by both continuous and discrete predictors and therefore we adopted a Bayesian Generalized Linear Model approach.

Rational for covariate inclusion and Directed Acyclic Graph (DAG)

We considered all the potential environmental variables which could affect the abundances of both *V. velutina* and *V. crabro*:

- the median Normalized Difference Vegetation Index (NDVI), calculated using the seventh and the eighth bands of multi-spectral Sentinel-2 satellite imageries (https://theia.cnes.fr). The median NDVI was calculated to account for the landscape and the presence of a forest cover, which is important for the two species, as tree trunks and branches are adopted as sites for nest construction (e.g. *V. crabro*, Matsuura, 1991, secondary nests of *V. velutina*, Franklin *et al.*, 2017) and as foraging areas. A high value of the NDVI index therefore would correspond to forested areas, whereas a low value of the NDVI would correspond to urbanised or agricultural areas;
- the average number of nests of *V. velutina* around the traps between 2016 and 2018, to account for two possible dynamics. On the one hand, if a certain trap was located in proximity of an area with stable nests of *V. velutina*, it was more likely that it would have caught more individuals of that species, which for example were moving for foraging. On the other hand, as the two species are expected to compete, it is plausible some sort of long-term spatial segregation, where areas with nests of *V. velutina* are characterized by the absence of nests of *V. crabro*, and a lower number of individuals of this latter species that would have been caught. Nest positions were retrieved from activities of the LIFE STOPVESPA project (https://www.vespavelutina.eu) and the monitoring network previously described by the authors (Lioy *et al.*, 2019). It is important to note that we did not measured the average number of nests of *V. crabro*, as there was no dedicated monitoring schema, but nevertheless as we hypothesized some exclusion between the two species in terms of nesting sites, this was not deemed to be necessary;
- the median slope of the terrain around the traps, as this could have affected the NDVI, with steeper areas being characterized by woodlands, and lowlands occupied by urbanized and farmland areas. This variable is also influencing the distance from water, with steep areas being closer to water bodies. The slope was determined from a digital elevation model (DEM) at 25 m of resolution (https://land.copernicus.eu);

- the median aspect of the terrain around the traps, as this could have affected the NDVI, with areas with different exposure being characterized by different land covers, the presence of olive groves and also eventually by a different distance from water bodies, due to the directionality of rivers;
- the elevation of the traps, as this could have affected the NDVI, the average number of *V. velutina* nests, and the presence of *V. velutina* and *V. crabro*, which have altitude limits (Bertolino *et al.*, 2016; Monceau & Thiéry, 2017; Rodríguez-Flores *et al.*, 2019);
- the Euclidean distance between the trap and the nearest water body, as both *V. velutina* and *V. crabro* need water for their metabolism and nest construction (Bessa *et al.*, 2016), and could use these areas as nesting sites;
- the average density of honey bee colonies in the municipalities where the traps were located, as bees constitute the main food source for the two species and it is likely that areas with many honey bee colonies would have been more frequented by the two species, resulting into a higher number of catches. This data (https://www.vetinfo.it) was not considered at the trap level but at the municipality level, due to data access restrictions;
- the area covered by olive groves around the traps, as olive groves could have been exploited as foraging sites by the two species, due to their importance for native pollinators in Mediterranean ecosystems (Nielsen *et al.*, 2011; Martínez-Núñez *et al.*, 2020) and as nesting sites;
- the diversity of land cover types around the area calculated as the Rao's diversity index (Rao, 1982). The diversity of agroforest land cover is fundamental for insect biodiversity and the presence of pollinators (Medeiros *et al.*, 2019).

The model, represented as a Directed Acyclic Graph, is represented in Fig S.2. It was identified with the software Dagitty (www.dagitty.net).

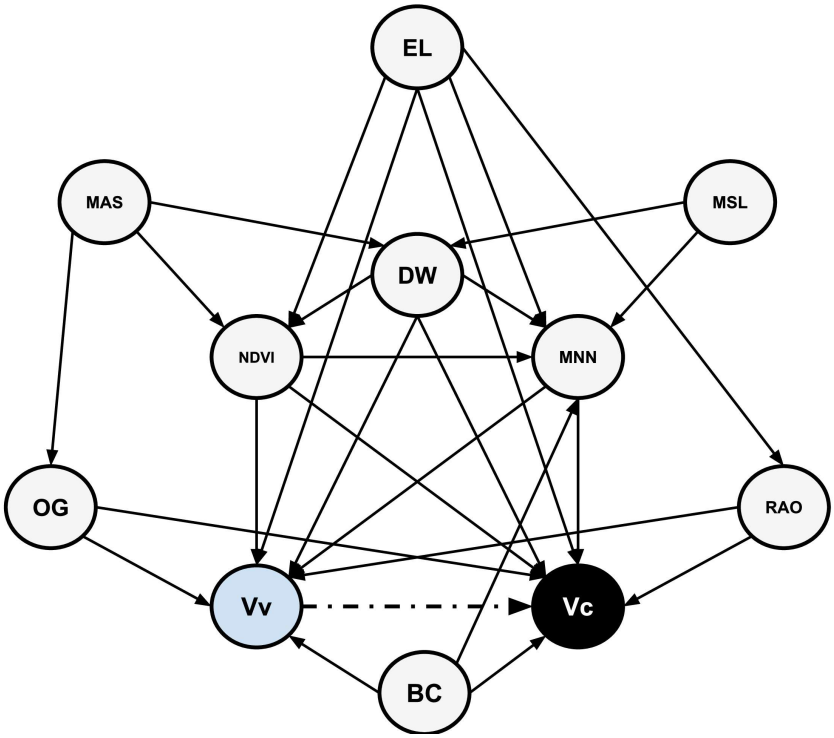

Fig. S.2 – Outline of the Directed Acyclic Graph of the model for explaining the relationship between *V. velutina*, *V. crabro* and the confounders. Arrows indicate causal effects between variables, represented as circles: Vv = Abundance of *V. velutina*, Vc = Abundance of *Vespa crabro*, BC = Mean density of honey bee colonies, NDVI = median of the Normalized Difference Vegetation Index, MNN = Mean number of nests of *V. velutina* over the previous three years, OG = Olive groves, RAO = Rao's diversity index, DW = Distance from water bodies, MSL = Median slope, MAS = Median aspect, EL = elevation. The causal effect of interest is Vv → Vc, represented as a dashed arrow. By controlling for all confounders (light circles), Vv → Vc was identified.

To account for the fact that both *V. velutina* and *V. crabro* can move for foraging or other activities, NDVI, the average number of nests, median slope and aspects, olive groves coverage and land cover diversity were calculated over a 500 m radius around the traps. This radius, based on previous knowledge about the movement ecology of the two species (Ugolini, Kesller, & Ishay, 1987; Poidatz *et al.*, 2018), was deemed sufficient to correctly represent the confounding effect of these variables.

Model structure and outcomes

Considered the distribution of our response variable (Fig. S.3), representing the number of *V. crabro* caught per day per trap, we opted for a Gamma distribution of the error term. Our

model was implemented with brms (Bürkner, 2016), an interface for the STAN software (Carpenter *et al.*, 2017) and it was based on Bayesian inference.

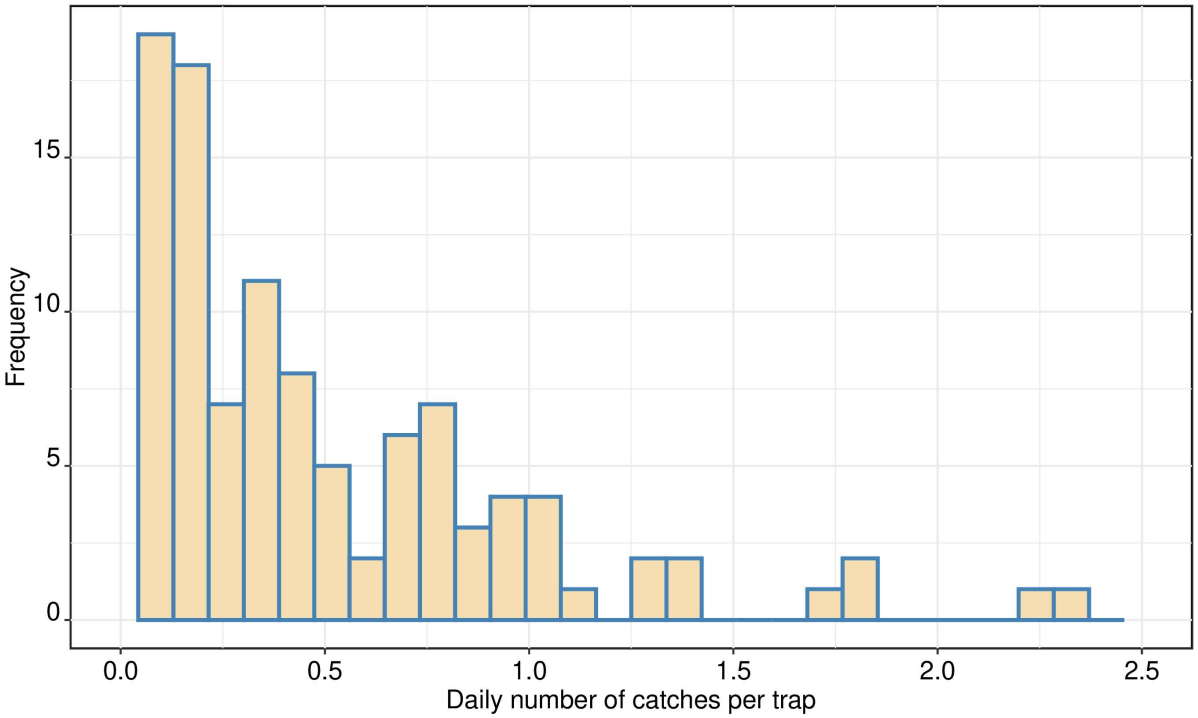

Fig. S.3 – Distribution of the daily number of individuals of *V. crabro* caught per trap.

We run four Markov Chain Monte Carlo chains with 5000 iterations each and a burn-in of the first 1000 observations. A complete outline of model fitting, including the exploration of its residuals for choosing the functional forms of the predictors, is available in the Reproducible Software Code, however our best candidate model had two characteristics, compared to the initial linear regression:

- it adopted a quadratic polynomial term for modelling the effect of the abundance of *V. velutina* on *V. crabro*, as well as for the confounding effects of NDVI, slope and aspect;
- it adopted a distributional approach, as we also modelled the shape parameter, representing the variability in our data in function of the abundances of *V. velutina* (Bürkner, 2017). This approach was adopted, as we noticed an increasing heterogeneity in the abundances of *V. crabro*, for increasing abundances of *V. velutina*, and it helped us improving model estimates.

Following Lemoine (2019), we specified the prior distribution of model coefficients, as a normal distribution with mean equal to 0 and variance equal to 1. As the effect of the abundance of *V. velutina* over *V. crabro* is non-linear, we should plot the marginal effect, to better appreciate the relationship (Fig. S.4).

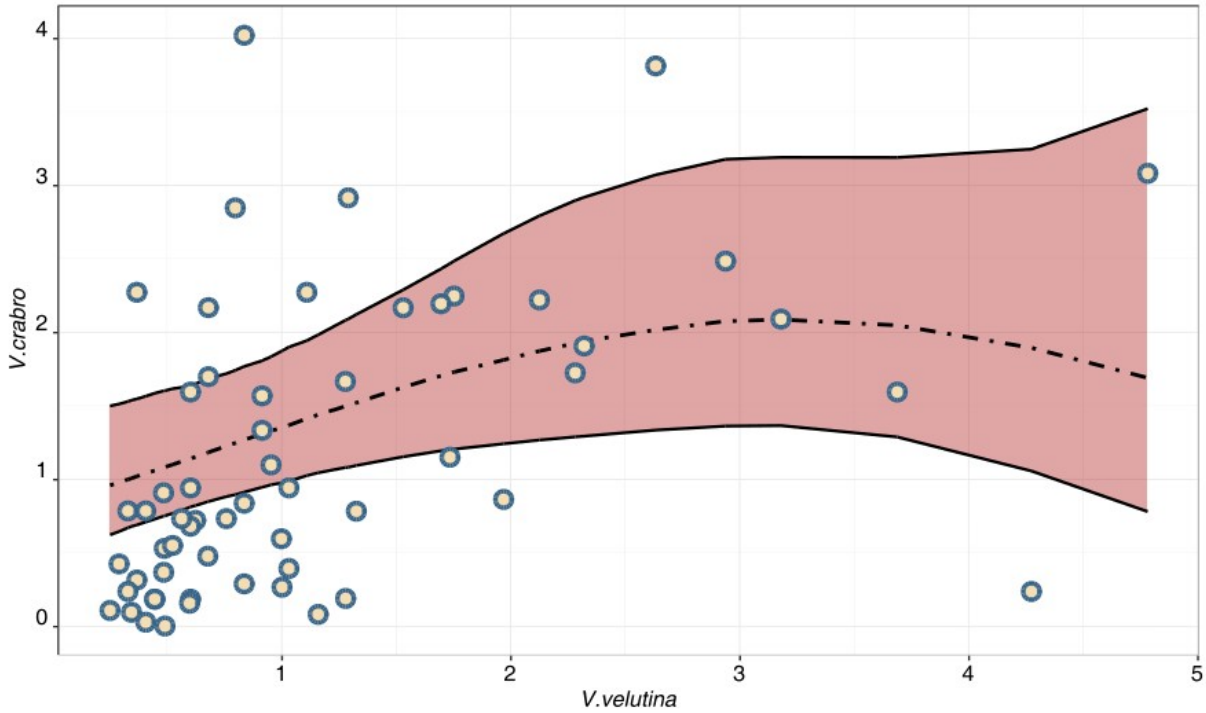

Fig. S.4 – Marginal effect of the abundance of *V. velutina* over the abundance of *V. crabro*. The 95% confidence interval is highlighted in red.

Diagnostics

Now we could explore the pattern of the residuals versus the fitted values of the model. Ideally, including every relevant covariates (and every potential confounding effects) in the model, no particular pattern should be detected in the scatterplot (Fig. S.5).

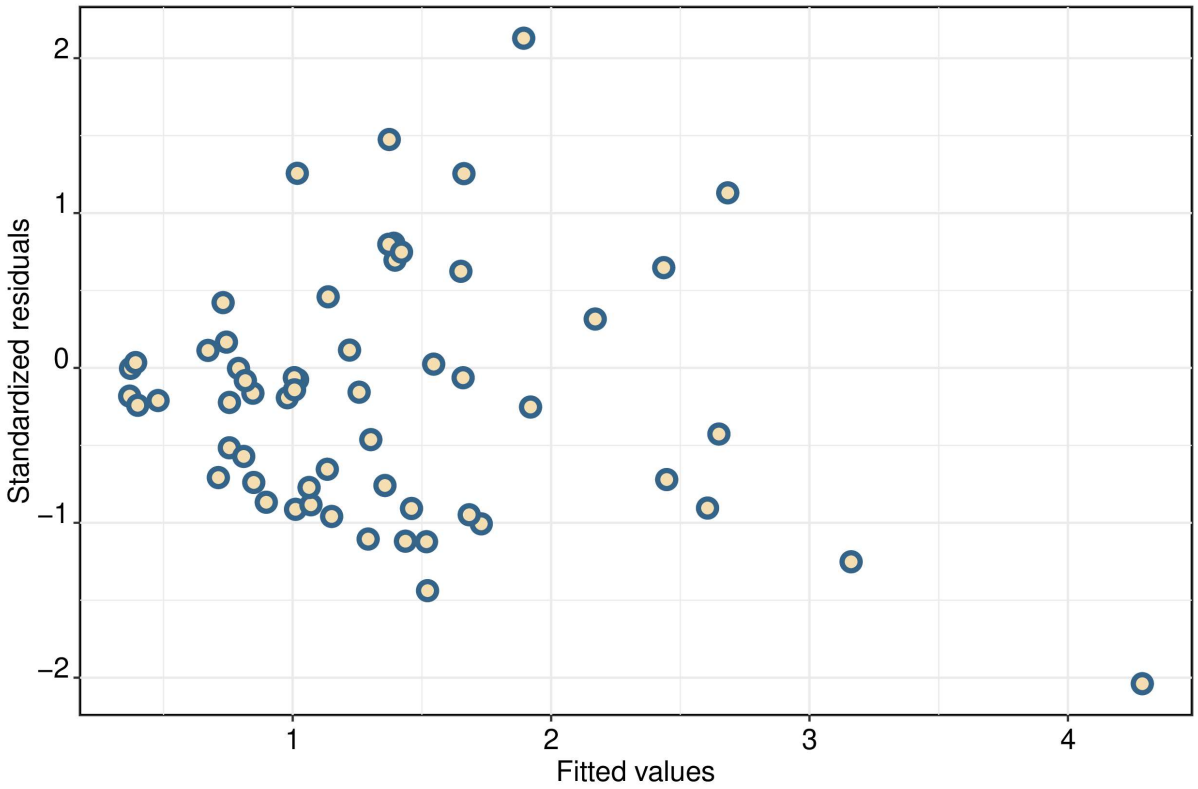

Fig. S.5 – Standardized residuals versus fitted values of the model for detecting the effect of the abundance of *V. velutina* over *V. crabro*: no clear pattern due to missing covariates are detected.

We can also explore spatial correlation between Moran's semivariogram, using model residuals and the coordinates of the trapping sites. Following Zuur (2012), the variogram can be computed by:

- calculating the Euclidean distance between trapping sites;
- taking all the combinations of sites *i* and *j*, that are separated by a certain distance *d*, and calculate the squared difference of model residuals at *i* and *j*;
- averaging squared difference of model residuals for all the combinations of trapping stations at the same distance *d*;
- repeat the process for all the distances;
- plot average squared differences versus the distance in kilometres between sites.

In our case, we selected 1 km distance belts, between 1 and 18 km, which is the maximum distance between trapping sites. No clear pattern emerges from this analysis (Fig. S.6), suggesting the absence of isotropic spatial correlation between observations.

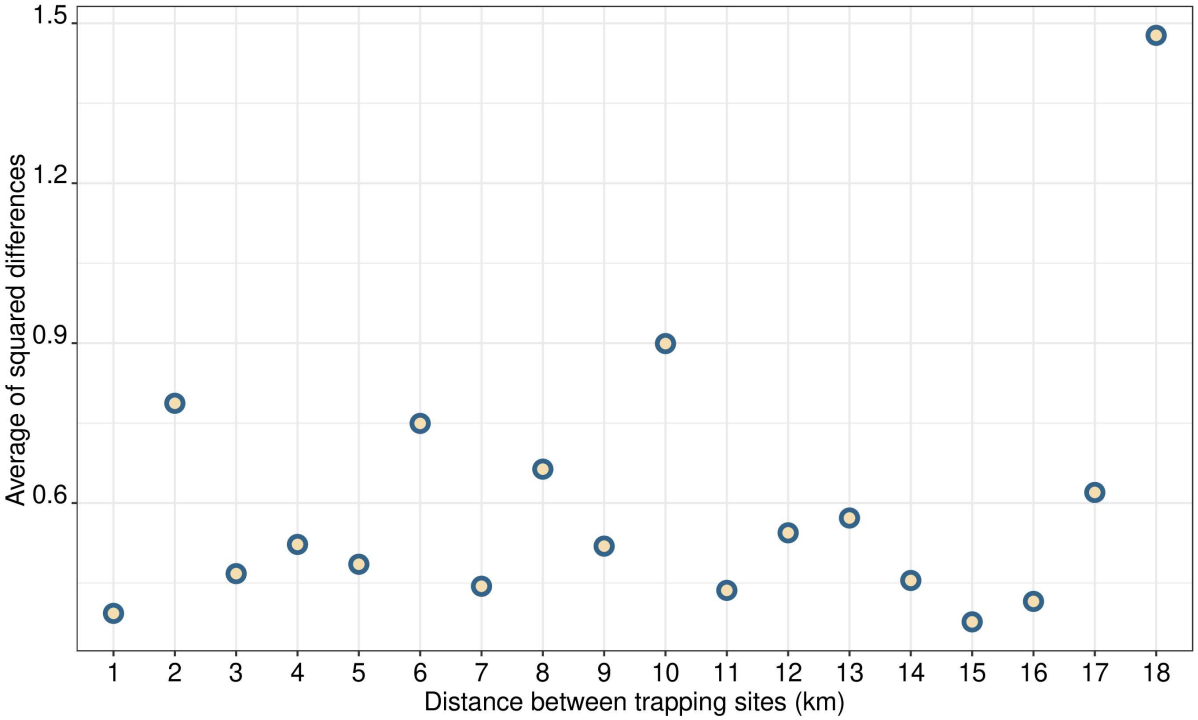

Fig. S.6 – Variogram of the model for detecting the effect of the abundance of *V. velutina* over *V. crabro*: average difference of squared residuals, for each distance class, versus distances between sampling points.

Our candidate model does not appear to be affected by spatial correlation, nor to have any strange patterns in model residuals and this might suggest that we successfully address all relevant covariates. At worst, we are over-controlling and losing in terms of model predictions. However, we are reasonably sure not to have forgotten any major confounder.

Cluster analysis between study sites

In this section, we will show how we carried out a k-means cluster analysis, to demonstrate that there are no significantly different groups of trapping sites between the two study areas, which differ for *V. velutina* presence. This comparison was performed using the environmental covariates adopted in the model explained above, which we assume are relevant also for *Vespula vulgaris* and *Vespula germanica*. In the case the two sites would have similar environmental conditions, the density of native Vespidae could be compared. On the other hand, in the case of a heterogeneous distribution between the two sites, we could not claim the Vespidae density to be comparable, as the two valleys are likely to have different environmental conditions.

We used the silhouette width method to identify the optimal number of clusters (Fig. S.7), which is two of them.

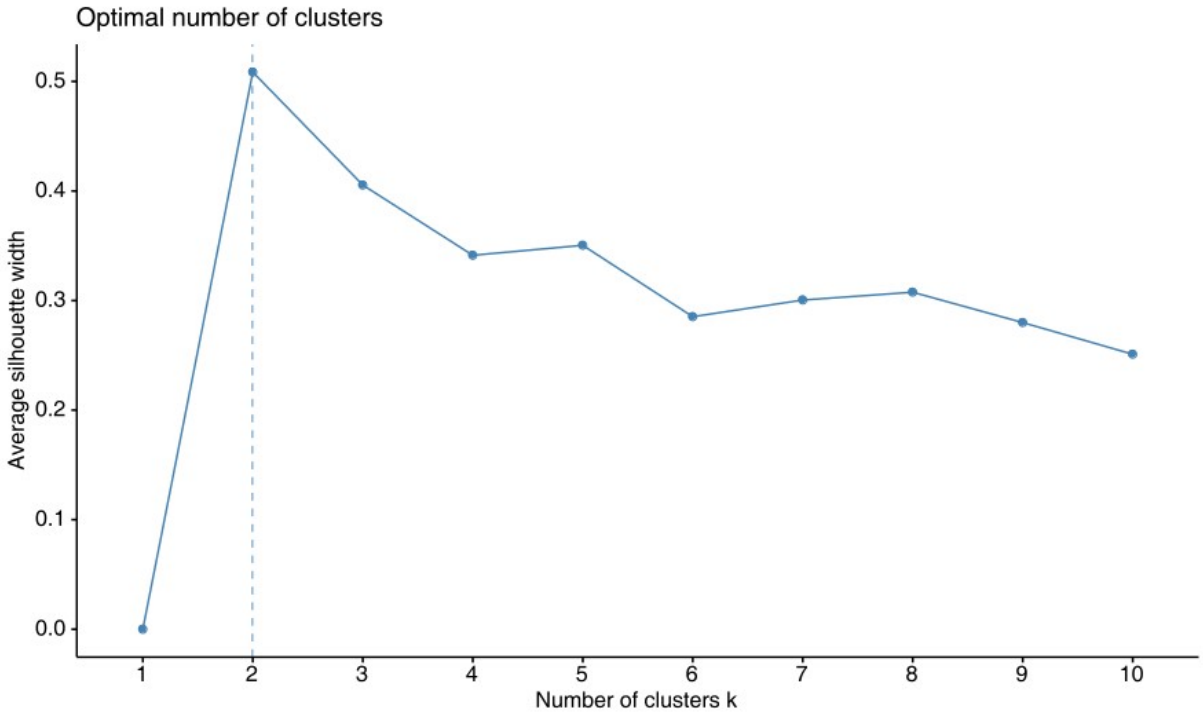

Fig. S.7 – Output of the silhouette width method for identify the optimal number of clusters. See Kassambara (2017) for further details about the method.

By fitting a k-means cluster analysis, with two clusters, we noticed that there were two groups of trapping stations with different environmental conditions, corresponding to areas with higher or lower values of the NDVI (woodlands versus croplands and urbanized areas, see the Reproducible R code; Fig. S.8).

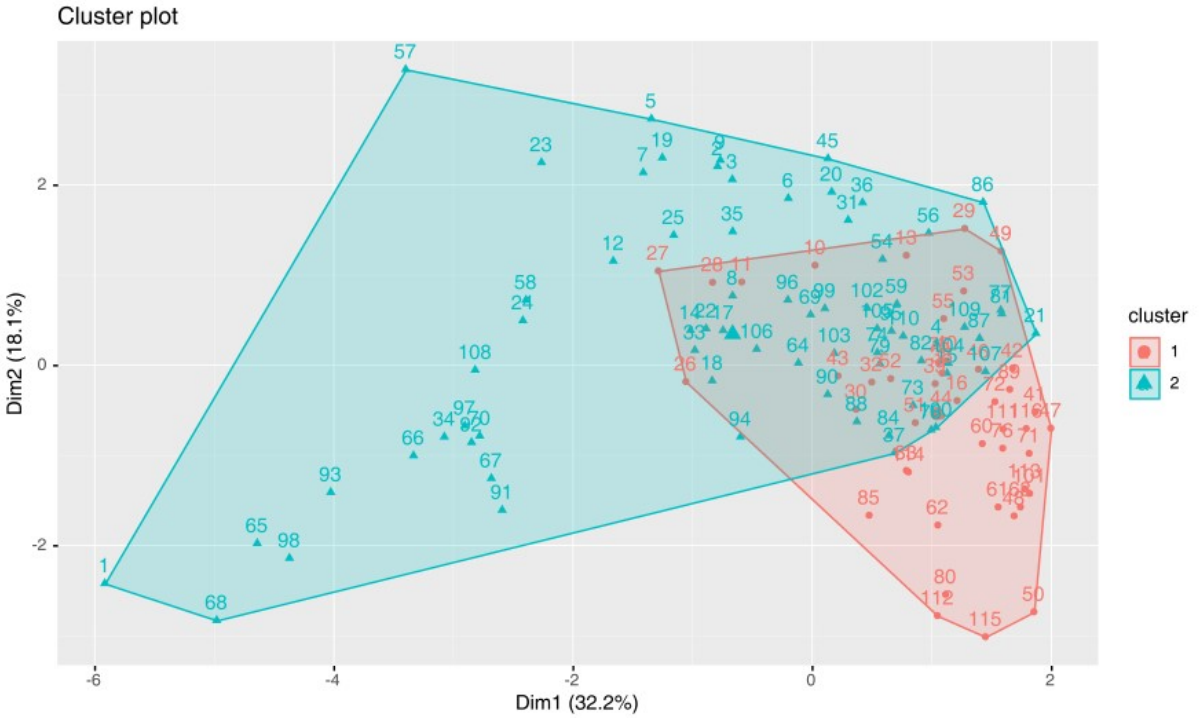

Fig. S.8 – Output of the k-means cluster analysis, with the two clusters.

However, the distribution of the two clusters of observations did not differed markedly between the two valleys. Trapping sites from cluster 1 and 2 did not differed between the invaded (cluster 1 = 57.8%, cluster 2 = 45.0%) and the non-invaded valley (cluster 1 = 42.2%, cluster 2 = 54.9%). Considered that the proportions were relatively similar and that the two groups of clusters also had a certain overlap, we concluded that the environmental conditions between the two valleys were comparable.

References

Bertolino, S., Lioy, S., Laurino, D., Manino, A., & Porporato, M. (2016). Spread of the invasive yellow-legged hornet *Vespa velutina* (Hymenoptera: Vespidae) in Italy. *Appl. Entomol. Zool.* **51**, 589–597.

Bessa, A. S., Carvalho, J., Gomes, A., & Santarém, F. (2016). Climate and land-use drivers of invasion: predicting the expansion of *Vespa velutina nigrithorax* into the Iberian Peninsula. *Insect Conserv. Divers.* **9**, 27–37.

Bollen, K.A., & Pearl, J. (2013). Eight myths about causality and structural equation models. In *Handbook of causal analysis for social research*: 301-328. Dordrecht: Springer.

Bürkner, P.C. (2016). brms: an R package for bayesian generalized linear mixed models using Stan. *J. Stat. Softw*. **22**.

Bürkner, P.C. (2017). Advanced Bayesian multilevel modeling with the R package brms. *arXiv preprint*, **1705.11123**.

Carpenter, B., Gelman, A., Hoffman, M. D., Lee, D., Goodrich, B., Betancourt, M., Brubaker, M., Guo, J., Li, P., & Riddell, A. (2017). Stan: A probabilistic programming language. *J. Stat. Softw.* **76**.

Dunning, T. (2012). *Natural experiments in the social sciences: a design-based approach*. Cambridge: Cambridge University Press.

Franklin, D. N., Brown, M. A., Datta, S., Cuthbertson, A. G. S., Budge, G. E., & Keeling, M. J. (2017). Invasion dynamics of Asian hornet, *Vespa velutina* (Hymenoptera: Vespidae): a case study of a commune in south-west France. *Appl. Entomol. Zool.* **52**, 221–229.

Kassambara, A. (2017). *Practical guide to cluster analysis in R: unsupervised machine learning*. Vol. 1. Sthda.

Lemoine, N. P. (2019). Moving beyond noninformative priors: why and how to choose weakly informative priors in Bayesian analyses. *Oikos* **128**, 912-928.

Lioy, S., Manino, A., Porporato, M., Laurino, D., Romano, A., Capello, M., & Bertolino, S. (2019). Establishing surveillance areas for tackling the invasion of *Vespa velutina* in outbreaks and over the border of its expanding range. *NeoBiota* **69**, 51–69.

Martínez-Núñez, C., Manzaneda, A. J., Isla, J., Tarifa, R., Calvo, G., Molina, J. L., Salido, T., Ruiz, C., Gutiérrez, J. E., & Rey, P. J. (2020). Low-intensity management benefits solitary bees in olive groves. *J. Appl. Ecol.* **57**, 111–120.

Matsuura, M. (1991). Vespa and Provespa. In *The social biology of wasps*: 232–262. New York: Cornell University Press New York.

Medeiros, H. R., Martello, F., Almeida, E. A. B., Mengual, X., Harper, K. A., Grandinete, Y.

C., Metzger, J. P., Righi, C. A., & Ribeiro, M. C. (2019). Landscape structure shapes the diversity of beneficial insects in coffee producing landscapes. *Biol. Conserv.* **238**, 108193.

Monceau, K., & Thiéry, D. (2017). *Vespa velutina* nest distribution at a local scale: an 8-year survey of the invasive honeybee predator. *Insect Sci.* **24**, 663–674.

Morgan, S.L & Winship, C., (2015). *Counterfactuals and causal inference*. Cambridge: Cambridge University Press.

Nielsen, A., Steffan-Dewenter, I., Westphal, C., Messinger, O., Potts, S. G., Roberts, S. P. M., Settele, J., Szentgyörgyi, H., Vaissière, B. E., Vaitis, M., Woyciechowski, M., Bazos, I., Biesmeijer, J. C., Bommarco, R., Kunin, W. E., Tscheulin, T., Lamborn, E., & Petanidou, T. (2011). Assessing bee species richness in two Mediterranean communities: importance of habitat type and sampling techniques. *Ecol. Res.* **26**, 969–983.

Poidatz, J., Monceau, K., Bonnard, O., & Thiéry, D. (2018). Activity rhythm and action range of workers of the invasive hornet predator of honeybees *Vespa velutina*, measured by radio frequency identification tags. *Ecol. Evol.* **8**, 7588–7598.

Rao, C. R. (1982). Diversity and dissimilarity coefficients: a unified approach. *Theor. Popul. Biol.* **21**, 24–43.

Rodríguez-Flores, M. S., Seijo-Rodríguez, A., Escuredo, O., & Seijo-Coello, M. del C. (2019). Spreading of *Vespa velutina* in northwestern Spain: influence of elevation and meteorological factors and effect of bait trapping on target and non-target living organisms. *J. Pest Sci.* **92**, 557–565.

Ugolini, A., Kesller, A., & Ishay, J. S. (1987). Initial orientation and homing by oriental hornets, *Vespa orientalis* L. (Hymenoptera Vespidae). *Monit. Zool. Ital. J. Zool.* **21**, 157–164.

Zuur, A. F. (2012). *A beginner's guide to generalized additive models with R.* Newburgh. New York: Highland Statistics Limited.